2002

Development and characterization of a reconstituted yeast translation initiation system

Mikkel A. Algire

David Maag

Peter Savio

Michael G. Acker

Salvador Z. Tarun Jr.

See next page for additional authors

Recommended Citation

Algire M.A., Maag D., Savio P., Acker M.G., Tarun Jr. S.Z., Sachs A.B., Asano K., Nielsen K.H., Olsen D.S., Phan L., Hinnebusch A.G., Lorsch J.R. (2002) Development and characterization of a reconstituted yeast translation initiation system. RNA 8: 382-397. doi: 10.1017/S1355838202029527

RNA (2002), *8*:382–397. Cambridge University Press. Printed in the USA.

DOI: 10.1017.S1355838202029527

METHOD

Development and characterization of a reconstituted yeast translation initiation system

MIKKEL A. ALGIRE,[1,6] DAVID MAAG,[1,6] PETER SAVIO,[1] MICHAEL G. ACKER,[1] SALVADOR Z. TARUN, JR.,[2] ALAN B. SACHS,[2] KATSURA ASANO,[3,4] KLAUS H. NIELSEN,[3] DEANNE S. OLSEN,[3] LON PHAN,[3,5] ALAN G. HINNEBUSCH,[3] and JON R. LORSCH[1]

[1]Department of Biophysics and Biophysical Chemistry, Johns Hopkins University School of Medicine, Baltimore, Maryland 21205, USA
[2]Department of Molecular and Cell Biology, University of California at Berkeley, Berkeley, California 94720, USA
[3]Laboratory of Eukaryotic Gene Regulation, National Institute of Child Health and Human Development, National Institutes of Health, Bethesda, Maryland 20892, USA

ABSTRACT

To provide a bridge between in vivo and in vitro studies of eukaryotic translation initiation, we have developed a reconstituted translation initiation system using components from the yeast *Saccharomyces cerevisiae*. We have purified a minimal set of initiation factors (eIFs) that, together with yeast 80S ribosomes, GTP, and initiator methionyl-tRNA, are sufficient to assemble active initiation complexes on a minimal mRNA template. The kinetics of various steps in the pathway of initiation complex assembly and the formation of the first peptide bond in vitro have been explored. The formation of active initiation complexes in this system is dependent on ribosomes, mRNA, Met-tRNA$_i$, GTP hydrolysis, eIF1, eIF1A, eIF2, eIF5, and eIF5B. Our data indicate that eIF1 and eIF1A both facilitate the binding of the eIF2•GTP•Met-tRNA$_i$ complex to the 40S ribosomal subunit to form the 43S complex. eIF5 stimulates a step after 43S complex formation, consistent with its proposed role in activating GTP hydrolysis by eIF2 upon initiation codon recognition. The presence of eIF5B is required for the joining of the 40S and 60S subunits to form the 80S initiation complex. The step at which each of these factors acts in this reconstituted system is in agreement with previous data from in vivo studies and work using reconstituted mammalian systems, indicating that the system recapitulates fundamental events in translation initiation in eukaryotic cells. This system should allow us to couple powerful yeast genetic and molecular biological experiments with in vitro kinetic and biophysical experiments, yielding a better understanding of the molecular mechanics of this central, complex process.

Keywords: eIF; eukaryotic initiation factor; kinetics; mechanism; mRNA; ribosome; tRNA

INTRODUCTION

Translation initiation in eukaryotes is an exquisitely complex process involving the action of over 20 non-ribosomal polypeptides and the hydrolysis of both GTP and ATP. In the current model for the events required for the formation of an initiation complex (Hershey & Merrick, 2000), the initiator methionyl-tRNA (Met-tRNA$_i$) is bound by the eukaryotic initiation factor 2-GTP complex (eIF2•GTP) to form a ternary complex. This ternary complex then binds to the small (40S) ribosomal subunit to form a 43S complex. The 43S complex can then bind to the 5′ end of the mRNA near the 7-methylguanosine cap structure. This step is facilitated by the eIF4F complex, made up of the cap-binding protein eIF4E, the RNA-dependent ATPase, and putative RNA helicase eIF4A and a multifaceted RNA- and initiation factor-binding protein called eIF4G. This complex is thought to unwind structured regions in the 5′ untranslated region (UTR) of the mRNA facilitating the binding of the 43S complex. A second

Reprint requests to: Jon Lorsch, Department of Biophysics and Biophysical Chemistry, Johns Hopkins University School of Medicine, 725 N. Wolfe Street, Baltimore, Maryland 21205-2185, USA; e-mail: jlorsch@jhmi.edu.
[4]Present address: Division of Biology, Kansas State University, Manhattan, Kansas 66506, USA.
[5]Present address: National Center for Biotechnology Information/ National Library of Medicine, National Institutes of Health, Bethesda, Maryland 20892, USA.
[6]These authors contributed equally to this work.

multisubunit complex, eIF3, is thought to be bound to the 40S ribosomal subunit prior to binding of the ternary complex and has been proposed to promote both the binding of the 43S complex to the mRNA and the initial formation of the 43S complex itself. Once the 43S complex is bound to the 5′ end of the mRNA, it is thought to scan along the mRNA looking for an AUG initiation codon. When it finds the initiation codon, a signal is transduced to eIF2, which hydrolyzes its bound GTP in a process stimulated by eIF5, the GTPase activating protein for eIF2. At this stage the eIF2•GDP complex can dissociate from its binding site on the small ribosomal subunit, leaving Met-tRNA$_i$ behind, presumably bound to the small subunit's P-site. The eIF2•GDP complex is recycled through the action of the GDP:GTP exchange factor eIF2B. Following eIF2•GDP dissociation from the 40S•mRNA•Met-tRNA$_i$ complex, the large (60S) ribosomal subunit is joined to the small subunit in a reaction catalyzed by a second GTPase initiation factor, eIF5B. Once subunit joining is complete, eIF5B hydrolyzes its bound GTP and dissociates from the newly formed 80S initiation complex. This complex can then bind a second aminoacyl-tRNA in its A-site, a process mediated by elongation factor 1α, and the first peptide bond can be formed.

We recently set out to test and further refine this model by dissecting the initiation process kinetically. Our initial studies employed a semipurified mammalian system (Lorsch & Herschlag, 1999). This system allowed us to develop the methods necessary for a quantitative dissection of the initiation process and allowed us to probe a number of the key steps on the pathway to initiation complex formation. However, to explore fully the molecular mechanics of eukaryotic translation initiation using these approaches, we felt a completely reconstituted system was required in which the concentrations and structures of every component could be independently varied. Reconstituted systems based on mammalian components have existed for over 20 years (Trachsel et al., 1977; Benne & Hershey, 1978), but we reasoned that in vitro reconstitution of yeast translation initiation would be an important complement to these mammalian systems because the power of yeast genetics and molecular biology could be directly coupled to the biochemical and biophysical approaches possible in vitro.

We report here the development and characterization of a minimal reconstituted translation initiation system using components from the yeast *Saccharomyces cerevisiae*. Central events of the initiation process—ternary complex formation, 43S complex formation, initiation codon recognition, subunit joining, and peptide bond formation—are recapitulated in the system. The assembly of 43S and 80S complexes depends strongly on a core group of initiation factors, and our data support many of the previously proposed roles for these factors. We have also probed the kinetics of several of the key steps in the initiation pathway in this in vitro system, supporting the feasibility of a complete kinetic and thermodynamic dissection of the initiation process using the system. We believe that this system will allow advances in our understanding of the molecular mechanics of eukaryotic translation initiation by providing a bridge between in vivo and in vitro studies.

RESULTS

The components of the system

We set out to reconstitute yeast translation initiation in vitro using purified components. As a starting point for these studies, we have purified a minimal set of *S. cerevisiae* translation initiation factors (eIFs). To achieve high yields and purity, initiation factors comprised of single subunits (eIF1, eIF1A, eIF5, and a truncated form of eIF5B; see Materials and Methods) were overexpressed in and purified from *Escherichia coli.* In contrast, the multisubunit factors eIF2 and eIF3 were purified directly from *S. cerevisiae*. All factors, with the exception of eIF3, were purified to >95% purity based on Coomassie staining of SDS-PAGE gels (Fig. 1). Due to its multisubunit nature, the yield of eIF3 was considerably lower than those of the other factors, making an estimation of its purity by staining of SDS-PAGE gels difficult.

Salt-washed 80S ribosomes and 40S ribosomal subunits were purified from *S. cerevisiae* as described in Materials and Methods. To simplify the initial experiments, a minimal mRNA template was used (Lorsch & Herschlag, 1999; Materials and Methods). This RNA was a 43-mer that is mostly poly(UC) with an AUG codon in the middle (5′-GGAA[UC]$_7$UAUG[CU]$_{10}$C). Such a template is predicted to lack significant secondary and tertiary structure (Saenger, 1984). The lack of structure appears to obviate the need for events such as cap recognition and RNA unwinding, simplifying the initial development of the reconstituted system and the study of various steps involved in complex assembly at the AUG codon.

Optimization of reaction conditions

A set of optimized component concentrations was established using the methionyl-puromycin assay (described below) as a readout for initiation complex formation. To limit the reactions to a single turnover and simplify kinetic analysis, the labeled component of the system, ^{35}S-Met-tRNA$_i$, was included at a limiting concentration of 3 nM. The concentrations of the ribosomes, GTP, puromycin, the model mRNA, and each of the initiation factors were systematically varied to identify the optimum concentrations listed in Table 1. Simultaneously doubling all of the concen-

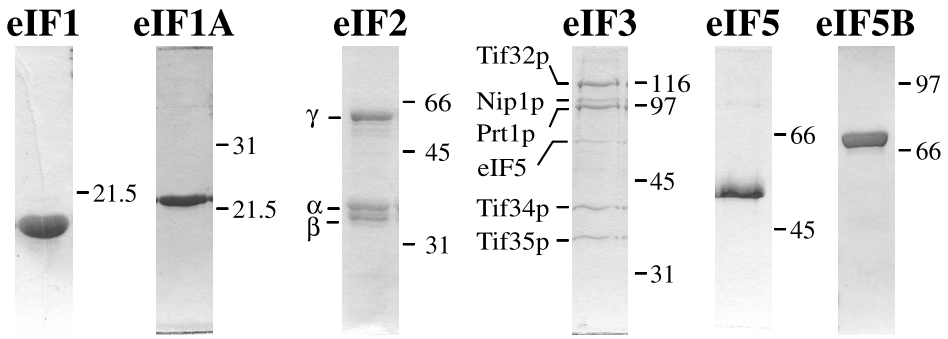

FIGURE 1. Purification of eukaryotic translation initiation factors (eIFs). Factors were purified as described in Materials and Methods. Purified factors were resolved by SDS-PAGE and visualized by staining with Coomassie brilliant blue. Positions of molecular weight markers (in kilodaltons) are indicated. In the eIF3 preparation the Tif32, Prt1, Tif34, Tif35, and eIF5 subunits were positively identified by western blotting.

trations shown in Table 1 did not significantly affect the rate of the reaction (data not shown), suggesting that these concentrations are saturating.

Further experiments were conducted to optimize the reaction buffer conditions. The rate of the reaction has a bell-shaped dependence on magnesium concentration, with maximal activity at a concentration of 3 mM (data not shown). Additionally, various monovalent ions (ammonium acetate, potassium chloride, and potassium acetate) were tested, and it was found that the system has maximum activity with 100 mM potassium acetate (data not shown). To ensure consistency and the highest levels of activity possible, all subsequent reactions were carried out at the concentrations listed in Table 1 and under the buffer conditions described in Materials and Methods.

Purified eIFs and ribosomes are competent to form 43S•mRNA and 80S complexes

Using purified eIFs and other necessary components (Table 1; Materials and Methods), 43S•mRNA (hereafter referred to as 43S complexes for simplicity) and 80S initiation complexes can be assembled using purified 80S ribosomes as a source of ribosomal subunits (Fig. 2).

Assembly of 43S and 80S complexes were followed using ^{35}S-labeled Met-tRNA$_i$. The complexes were resolved from each other and from free tRNA by electrophoresis on native 4% polyacrylamide gels, as described in Materials and Methods. By loading reactions directly onto running gels, assembly can be stopped at desired times due to entry of the complexes into the gel matrix (Lorsch & Herschlag, 1999). Time points as early as 30 s can be obtained accurately using this method, allowing the kinetics of complex formation to be followed (Lorsch & Herschlag, 1999).

Lanes 1 and 2 and lanes 15 and 16 of Figure 2 indicate that complex formation is dependent on the addition of both purified eIFs and salt-washed 80S ribosomes, respectively. The complete dependence on the presence of ribosomes in the reactions strongly suggests that the complexes observed are eIF-ribosome complexes rather than complexes of Met-tRNA$_i$ and eIFs. Figure 2, lanes 3 and 4 show that eIF2 alone is not sufficient to promote stable 43S complex formation. Addition of eIF1 or eIF1A with eIF2, however, leads to the formation of a complex migrating in the position expected for a 43S complex based on its migration in the mammalian system (Fig. 2, lanes 5–8; Lorsch & Herschlag, 1999). Formation of this complex was maximized when eIF1, eIF1A, and eIF2 were included in the reactions together and GDPNP (a hydrolysis-resistant analog of GTP) was used in place of GTP (Fig. 2, lane 10). It should be noted that although eIF5 was included in the reactions depicted in lanes 9 and 10 of Figure 2, subsequent experiments indicated that eIF5 has no effect on the rate of formation of the 43S complex in this system in the presence of GDPNP (Table 2).

In the current model for translation initiation, upon initiation codon recognition by the 43S complex, eIF5 stimulates the GTPase activity of eIF2 leading to GTP

TABLE 1. Optimized concentrations of components in the Met-Puro and/or 43S assays.

Component	Standard concentration
eIF1	1 μM
eIF1A	400 nM
eIF2	160 nM
eIF5	240 nM
80S ribosomes	200 nM
Model mRNA	1 μM
^{35}S-Met-tRNA$_i$	$\leq$3 nM[a]
Puromycin	1.5 mM
GTP	500 μM
GDPNP	1 mM

[a]3 nM total ^{35}S-Met-tRNA, a small fraction of which may be elongator rather than initiator tRNA.

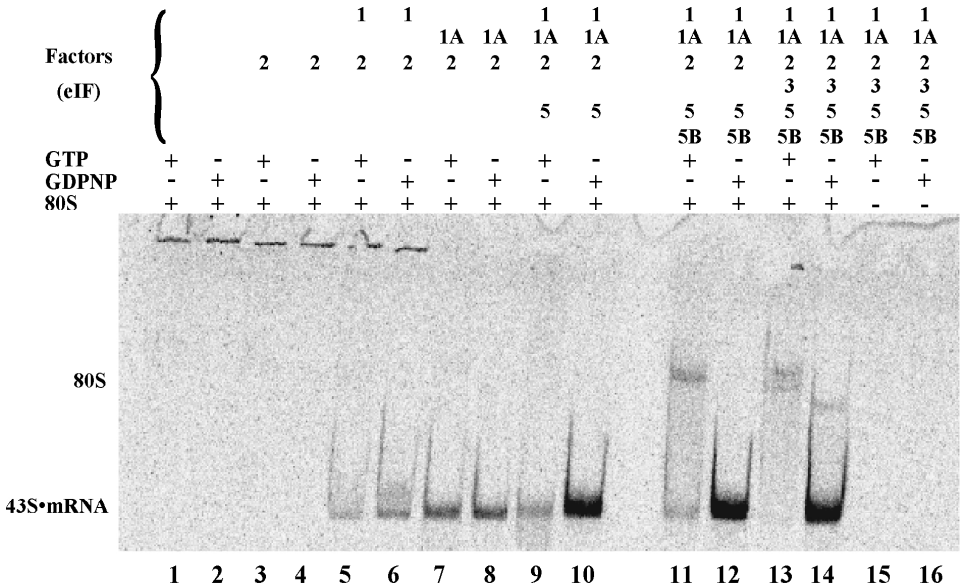

FIGURE 2. Phosphorimage of a native gel showing that 43S and 80S complexes can be assembled using purified yeast initiation factors and ribosomes. All reactions contained ^{35}S-Met-tRNA$_i$, model mRNA, and GTP or GDPNP (Table 1). Each reaction also contained initiation factors and salt-washed ribosomes as indicated at the top. Reactions were incubated at 26 °C for 30 min and then loaded onto a running native gel as described in Materials and Methods.

hydrolysis, dissociation of eIF1, eIF1A, and eIF2•GDP, and release of Met-tRNA$_i$ onto the 40S subunit (Hershey & Merrick, 2000). This step is followed by eIF5B-dependent joining of the 60S subunit to form an 80S initiation complex (Pestova et al., 2000). Consistent with this model, as shown in Figure 2, inclusion of eIF5B along with eIF5, eIF1, eIF1A, and eIF2 in reactions carried out in the presence of GTP leads to the formation of a higher molecular weight complex that migrates as expected for an 80S initiation complex (Fig. 2, lanes 11 and 13; Lorsch & Herschlag, 1999). In the presence of GDPNP, however, only the 43S complex is observed (Fig. 2, lane 12). This observation is consistent with at least one step requiring GTP hydrolysis on the pathway to 80S complex formation. Furthermore, eIF5 seems to destabilize the 43S complex in the presence of GTP and the absence of eIF5B (Fig. 2, compare lanes 7–10). We postulate that eIF5 is stimulating the hydrolysis of GTP by eIF2 and, because eIF5B is not present to promote subunit joining, Met-tRNA$_i$ slowly dissociates from the 40S•Met–tRNA$_i$•mRNA complex. In the presence of GDPNP, eIF5 does not destabilize the 43S complex, indicating that GTP hydrolysis is indeed required for this effect.

Interestingly, the inclusion of eIF3 in these reactions does not significantly affect the formation of 43S or 80S complexes (see next section, as well), although higher molecular weight complexes are observed in both cases, suggesting that the factor is at least capable of binding to 43S and 80S complexes (Fig. 2, lanes 14 and 13, respectively; although the levels of these higher molecular weight complexes are low, their presence when eIF3 is added to the reactions is highly reproducible; data not shown). Possible reasons for the lack of eIF3-dependence are discussed below.

TABLE 2. Observed (k_{obs})[a] and relative (k_{rel})[b] rate constants for 43S complex formation.

Omissions/additions	k_{obs} (min^{-1})	k_{rel}
Using 80S ribosomes		
None (control)[c]	0.39 ± 0.21	(1)
−eIF1	0.06 ± 0.03	0.15 ± 0.01
−eIF1A	0.006[d]	0.03[d]
−eIF1 and eIF1A	<0.002[e]	<0.01[e]
−eIF2	<0.002[e]	<0.01[e]
+eIF3	0.44[d]	1.2[d]
+eIF5	0.42[d]	1.2[d]
+eIF5B	0.36[d]	1.0[d]
Using 40S subunits		
None (control)[c]	1.17 ± 0.49	(1)
−eIF1	0.18[d]	0.11[d]
−eIF1A	<0.002[e]	<0.01[e]
−eIF1 and eIF1A	<0.002[e]	<0.01[e]
−eIF2	<0.002[e]	<0.01[e]

[a]Observed rate constants are averages of constants obtained in different experiments.

[b]Rate constant relative to rate constant from control reaction containing all components performed at the same time. The average k_{rel} from multiple independent determinations is given.

[c]Reaction contains eIF2, eIF1, and eIF1A.

[d]Experiment performed only once.

[e]Multiple experiments performed and all results below limit of detection.

Kinetics of 43S initiation complex formation can be monitored in the purified system

The typical experimental scheme for following 43S complex formation is shown in Figure 3A. Reactions were carried out with all of the components at saturating concentrations (Table 1) with the exceptions of the ^{35}S-Met-tRNA$_i$ (the limiting reagent) and any indicated omissions. By varying the incubation scheme and order of addition of components, different steps on the pathway to 43S complex formation can be monitored (Fig. 3B). The incubations P1 and P2 (Fig. 3A) are sufficient to allow complete formation of the eIF2•GDPNP•^{35}S-Met-tRNA$_i$ complex (hereafter referred to as ternary complex; ternary complex assembly was measured using nitrocellulose filter binding assays; L. Kapp & J.R. Lorsch, unpubl.; data not shown). Thus, depending on whether or not incubations P1 and P2 are carried out prior to initiating 43S formation by adding ribosomes, mRNA, and eIFs 1 and 1A, the kinetics of either ternary complex formation or the assembly of the ternary complex into the 43S complex can be examined. When reactions were initiated without preformation of the ternary complex, the observed rate constant for 43S complex formation was 20-fold lower than the observed rate constant for reactions initiated after ternary complex formation was complete (k_{obs} = 0.029 ± 0.004 min^{-1} and 0.58 ± 0.04 min^{-1}, respectively). This indicates that ternary complex formation is rate limiting in the absence of the P1 and P2 incubations. A number of independent experiments suggest that dissociation of GDP from eIF2 is the rate limiting step in ternary complex formation in this system (L. Kapp & J.R. Lorsch, unpubl. results; D. Maag, M. Algire, & J.R. Lorsch, unpubl. results). It is worth noting that this step is artificially slow in this system relative to what it would likely be in vivo because of the absence of eIF2B, a GTP:GDP exchange factor (Nika et al., 2000).

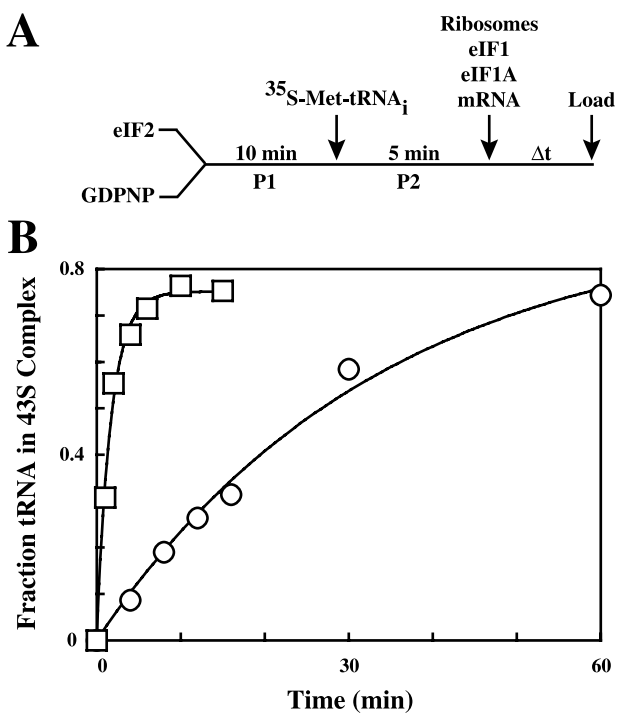

FIGURE 3. Measuring the kinetics of 43S complex formation. **A:** Typical experimental design. eIF2 is mixed with a saturating excess of GDPNP for 10 min to allow time for the slow exchange of eIF2-bound GDP for GDPNP (P1 phase). At that time, ^{35}S-Met-tRNA$_i$ is added and the mixture incubated for 5 min to allow ternary complex formation to proceed to completion (P2 phase). Ribosomes, model mRNA, eIF1, and eIF1A are then simultaneously added to initiate 43S complex formation. The reaction is allowed to proceed for some time (Δt), at which point an aliquot is removed, quickly mixed with 10× loading dye, and loaded onto a running native 4% polyacrylamide gel. **B:** Kinetics of reactions containing all components described in **A**. Reactions carried out following the P1 and P2 preincubations (□) proceeded at a 20-fold faster rate than reactions initiated without preformation of ternary complex (no P1 and P2 preincubations; ○). k_{obs} = 0.58 ± 0.04 min^{-1} and 0.029 ± 0.004 min^{-1}, respectively (errors given are errors of fits). The solid lines represent fits of the data with single exponentials.

The rationale for assembling the ternary complex in two separate steps (P1 and P2) came from the observation of significant ^{35}S-Met-tRNA$_i$ deacylation when the three components were mixed simultaneously and incubated. It has previously been reported that glycerol promotes the deacylation of charged tRNAs (Johnson & Adkins, 1984), and we found that the glycerol present in our reactions was indeed at least partially responsible for the observed significant deacylation of free Met-tRNA$_i$ (data not shown). This difficulty was overcome by allowing the slow exchange of GDP for GDPNP to proceed to completion (P1) before addition of ^{35}S-Met-tRNA$_i$ resulting in an eIF2•GDPNP complex that binds ^{35}S-Met-tRNA$_i$ rapidly (P2; data not shown) thereby minimizing the amount of time that the free tRNA is exposed to the glycerol in the buffer. Once bound to eIF2, the Met-tRNA$_i$ is apparently protected against deacylation (data not shown).

The amount of Met-tRNA$_i$ assembled into 43S complexes is typically around 80%, indicating that the majority of the ^{35}S-Met-tRNA$_i$ present in the reactions is competent for assembly. The remaining 20% could represent damaged Met-tRNA$_i$ or elongator Met-tRNA. The latter would be consistent with the observation that the *E. coli* methionyl-tRNA synthetase charges yeast elongator tRNA^{Met} with threefold lower efficiency than yeast initiator tRNA^{Met} under the charging conditions used (Rosa & Sigler, 1977). The kinetics of 43S complex formation are fit very well by a single exponential (Fig. 3B), suggesting the presence of only one active population of ribosomes and initiation factors.

The observed rate constant for 43S formation is not affected by omission of the model mRNA from the reactions. However, the endpoint of the 43S formation reaction is decreased two to threefold when the mRNA is omitted (data not shown), suggesting that the mRNA

stabilizes the binding of the ternary complex to the 40S subunit.

eIF1 and eIF1A accelerate the rate of 43S complex formation in the reconstituted system

The dependence of 43S complex formation on eIF1, eIF1A, and eIF2 are shown in a typical experiment in Figure 4. When salt-washed 80S ribosomes were used as the source of ribosomal subunits, omission of eIF1 or eIF1A individually resulted in a significant decrease in the rate of 43S complex formation (7-fold and 33-fold, respectively; Table 2). Omission of eIF1 and eIF1A together resulted in the complete loss of detectable complex formation (>100-fold less than the positive control). Similar results were obtained when eIF2 was omitted from the reactions. The presence of eIF5, eIF5B, or eIF3 did not affect the kinetics of 43S complex formation in this system (Table 2). Furthermore, these factors, either alone or in combination, could not rescue the effects of omitting eIF1 or eIF1A (data not shown).

When experiments were carried out using purified 40S subunits, similar results were obtained upon omission of eIF1, eIF1A, or eIF2, as were seen when 80S ribosomes were used (Table 2). However, the observed rate constant for 43S complex formation is approximately 3-fold greater when purified 40S subunits are used instead of 80S ribosomes. It is clear from the results in Table 2 that eIF1 and eIF1A both accelerate the rate of 43S complex formation, which is consistent with results obtained using mammalian systems (Trachsel et al., 1977; Benne & Hershey, 1978; Thomas et al., 1980a, 1980b; Chaudhuri et al., 1997, 1999).

80S complexes assembled from purified components can catalyze dipeptide bond formation

To examine whether or not the 80S complexes assembled in this system are active, we used methionyl-puromycin (Met-Puro) assays to monitor the formation of the first peptide bond. Figure 5A shows two different experimental protocols used to follow Met-Puro formation in the purified system. Similar to the experiment described in Figure 3A, preincubations P1 and P2 were used to assemble ternary complex prior to initiation of subsequent steps. It was necessary to use GTP rather than GDPNP in these experiments, however, because GTP hydrolysis is necessary during steps following 43S complex formation (e.g., by eIF2 and eIF5B). As can be seen in Figure 5B, Met-Puro is made when the reactions are carried out using either Scheme 1 or Scheme 2, indicating that the 80S complexes formed in this reconstituted system are active.

The kinetics of Met-Puro formation show a distinct lag phase (Fig. 5B, squares) when the reaction is carried out using Scheme 1 in which only the ternary complex is preformed prior to initiation of ribosomal complex formation and Met-Puro synthesis, indicating the presence of at least two slow steps between ternary complex assembly and Met-Puro formation. This lag phase is eliminated if a third incubation (P3) is performed with the remaining factors, ribosomes, and mRNA prior to addition of puromycin to initiate peptide bond formation

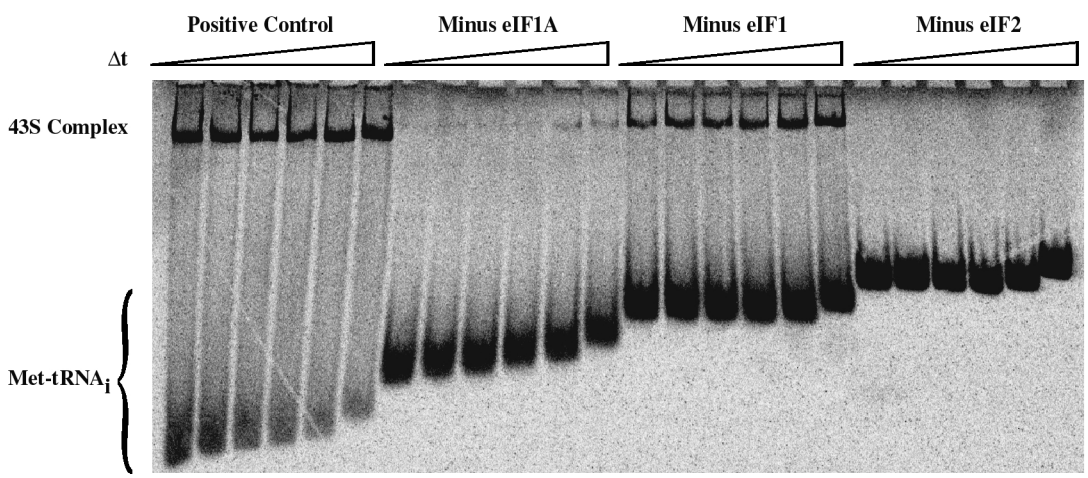

FIGURE 4. Phosphorimage of a native gel showing the effects of omitting eIF1, eIF1A, or eIF2 on 43S complex formation. All reactions were carried out exactly as described in Figure 3A (except for the indicated omissions) using purified 40S subunits. "Positive control" indicates that no component was omitted. Time courses were from 0.5 to 6 min. Observed and relative rate constants are included in Table 2. The staggering of the free ^{35}S-Met-tRNA$_i$ is due to the fact that the samples were loaded at different times onto a running gel. Free eIF2•GTP•Met-tRNA$_i$ complex apparently dissociates rapidly upon entering the gel (see Materials and Methods). The identity of the faint band just below the wells in some lanes is not known, but its presence is not consistent from experiment to experiment and thus it may be an aggregate of 43S complexes. It contains ≤5% of the amount of labeled tRNA present in the 43S band in all cases.

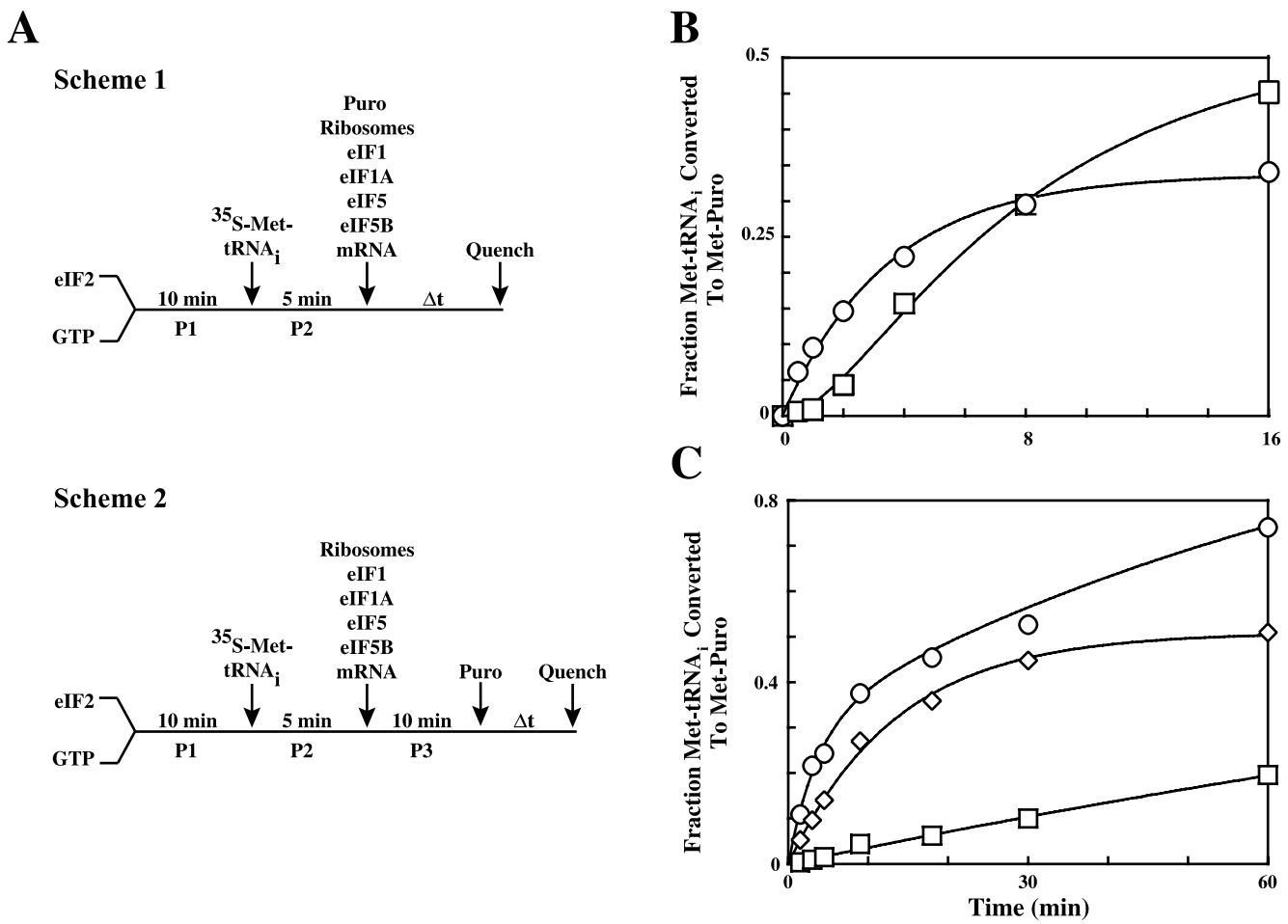

FIGURE 5. Measuring the kinetics of methionyl-puromycin formation. **A**: Two experimental designs. Scheme 1: Ternary complex formation is allowed to proceed to completion as described in Figure 3A (P1 and P2 phases). At that point, ribosomes, model mRNA, eIF1, eIF1A, eIF5, eIF5B, and puromycin are added simultaneously to initiate the remainder of complex formation and Met-Puro synthesis. Scheme 2: Following the P1 and P2 preincubations, ribosomes, model mRNA, eIF1, eIF1A, eIF5, eIF5B are added and the reaction incubated for an additional 10 min to allow the slow formation of intermediate complexes (P3 phase). Reactions are then initiated by the addition of puromycin, and aliquots removed and quenched at various times as described in Materials and Methods. **B**: Reactions initiated by simultaneous addition of puromycin with ribosomes, model mRNA, eIF1, eIF1A, eIF5, and eIF5B (Scheme 1; □) show a pronounced lag with respect to reactions carried out following the Scheme 2 preincubation protocol (○). Solid lines represent fits of the data with a single exponential (○) or an equation describing an irreversible, two-step process (□; see Materials and Methods). k_{obs} = 0.29 ± 0.02 min^{-1} (○), k_1 = 0.59 ± 0.26 min^{-1} and k_2 = 0.13 ± 0.04 min^{-1} (□). Errors given are errors of the fits. **C**: Effect of an unlabeled Met-$tRNA_i$ chase on the observed kinetics of Met-Puro formation. All experiments were performed using the Scheme 2 preincubation protocol. In the absence of the chase (○) the kinetics of formation of Met-Puro is fit very well with a double exponential (solid line) indicating at least two kinetic phases during the reaction. Addition of 88 nM unlabeled Met-$tRNA_i$ chase (◇) along with puromycin at the start of the Met-Puro formation reaction to prevent multiple reaction cycles resulted in the loss of the second kinetic phase. The resulting data are fit well with a single exponential (solid line). Addition of the unlabeled Met-$tRNA_i$ chase during the incubation of eIF2•GTP and ^{35}S-Met-$tRNA_i$ (□) resulted in the expected loss of signal.

(Fig. 5A, Scheme 2). This 10-min incubation allows for the slow formation of intermediate complexes in the initiation pathway, resulting in the observation of apparent first-order kinetics when peptide bond formation is initiated (Fig. 5B, circles).

When the reactions were followed for extended times, however, a second, slower phase was observed (Fig. 5C, circles). It seemed possible that this phase might be the result of recycling of a component of the system, resulting in additional rounds of ternary complex formation and eventually initiation complex formation. For example, 40S•mRNA•Met-$tRNA_i$ complexes might dissociate at a significant rate (e.g., Fig. 2, lane 9) and the free Met-$tRNA_i$ could then reenter the initiation process by forming a new ternary complex with eIF2•GTP. A similar dissociation pathway might also occur from the 80S•Met-$tRNA_i$ complex. To test this hypothesis, a chase of unlabeled Met-$tRNA_i$ (88 nM unlabeled vs. 3 nM labeled) was added along with the puromycin when peptide bond formation was initiated (Fig. 5C). The chase

of excess unlabeled Met-tRNA$_i$ should essentially prevent any further ternary complex formation involving ^{35}S-Met-tRNA$_i$. As a control, the unlabeled chase was added with the labeled Met-tRNA$_i$ at the start of the reaction (Fig. 5C, squares). As expected, this resulted in an apparent inhibition of Met-Puro formation (10-fold inhibition). In contrast, when the chase was added with the puromycin, only the second, slow phase of the reaction was inhibited, resulting in apparent first-order kinetics (Fig. 5C, diamonds). These results suggest that the second, slow phase requires additional rounds of ternary complex formation, although other models for the origin of this second phase cannot yet be ruled out. In any event, to ensure that single-turnover kinetics were being observed and to simplify the analysis of the data, the unlabeled Met-tRNA$_i$ chase was used in all subsequent experiments monitoring Met-Puro formation.

Dependence of active initiation complex formation on the components of the system

To test the dependence of active initiation complex formation on each of the components of the system, the kinetics of Met-Puro formation were followed under various conditions. Met-Puro formation is strongly dependent upon the addition of the model mRNA to the reaction, with reactions carried out in the absence of added mRNA proceeding approximately sevenfold slower than reactions carried out in the presence of saturating model mRNA (Table 3). The background level of Met-Puro synthesis is most likely due either to contaminating endogenous mRNA in the ribosome preparation or to template independent initiation events. The mRNA dependence of Met-Puro formation follows simple saturation kinetics (Fig. 6). When an RNA identical to the model mRNA but lacking the AUG codon was substituted for the model mRNA, the observed rate constant for Met-Puro formation was, within experimental error, identical to the observed rate constant when mRNA was omitted from the reactions (both AUG- and non-AUG-containing mRNAs present at 1 μM; Table 3). Poly(U) (1 μM in 43-mer units; heterogeneous length) also does not stimulate the formation of Met-Puro (data not shown). Thus, the formation of active initiation complexes in this system is dependent on both added mRNA and the presence of an AUG codon within the mRNA.

Observed rates of Met-Puro formation were also markedly decreased upon omission of eIF1, eIF1A, eIF2, or eIF5B, indicating that translation initiation in this purified system is dependent on all of these initiation factors (Table 3). As would be expected from the effects of component omissions on the kinetics of 43S complex formation (Table 2), omission of eIF2 or both eIF1 and eIF1A from Met-Puro experiments resulted in the loss of detectable Met-Puro formation ($k_{obs} < 0.002$ min^{-1}). Similar results were obtained when GTP was replaced with GDPNP. This is consistent with the observation that 80S complexes cannot assemble in the presence of GDPNP (Fig. 2) and with previous results indicating that there are at least two steps between ternary complex formation and peptide bond formation that require

TABLE 3. Observed (k_{obs})[a] and relative (k_{rel})[b] rate constants for Met-Puro assay.

Omissions or additions	k_{obs} (min^{-1})	k_{rel}
None (control)	0.21 ± 0.13[c]	(1)
−eIF1	0.028 ± 0.01	0.12 ± 0.02
−eIF1A	0.016 ± 0.01	0.10 ± 0.06
−eIF1 and eIF1A	<0.002[d]	<0.01[d]
−eIF2	<0.002[d]	<0.01[d]
+eIF3	0.30[e]	1.0[e]
−eIF5	0.13 ± 0.03	0.88 ± 0.17
−eIF5B	0.039 ± 0.02	0.11 ± 0.05
−Ribosomes	<0.002[e]	<0.01[d]
−Model mRNA	0.039 ± 0.03	0.14 ± 0.03
−AUG codon[f]	0.038[e]	0.11[e]
−GTP	0.013 ± 0.003	0.062 ± 0.02
+ GDPNP, −GTP	<0.002[d]	<0.01[d]
−Puromycin	<0.002[d]	<0.01[d]

[a]Observed rate constants are averages of constants obtained in different experiments.

[b]Rate constant relative to rate constant from control reaction containing all components performed at the same time. The average k_{rel} from multiple independent determinations is given.

[c]This is an average of 12 independent experimental values. The k_{rel} determined is relative to the control reaction from the same experiment, not this average k_{obs} value.

[d]Multiple experiments performed and all results below limit of detection.

[e]Experiment performed only once.

[f]The AUG containing model mRNA was replaced with 1 μM of an otherwise identical model mRNA except the AUG codon was replaced by UCU.

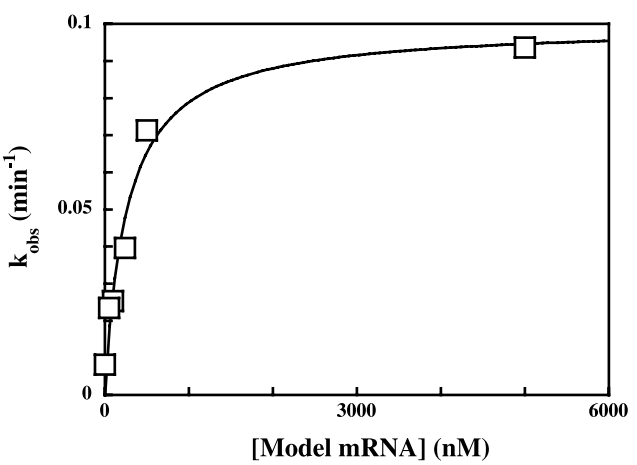

FIGURE 6. Initiation complex formation depends on the addition of model mRNA. Varying concentrations of model mRNA were used to obtain observed rate constants for Met-Puro synthesis in standard reactions (Table 1). The data are fit well with the Michaelis–Menten equation (solid line), giving an apparent K_m of 260 ± 70 nM and a maximum k_{obs} of 0.10 ± 0.01 min (errors given are errors of the fits).

GTP hydrolysis (Hershey & Merrick, 2000). The low level of activity observed when GTP was omitted but no GDPNP was added (Table 3) may be due to contaminating GTP in the ribosome or eIF2 preparations. Omission of eIF1 and eIF1A individually also resulted in significant reductions in the rate of Met-Puro formation (~10-fold for each; Table 3). Again, the dependence on these individual factors was in good agreement with results obtained in 43S complex formation experiments. Finally, omission of eIF5B resulted in a 10-fold decrease in the observed rate constant for Met-Puro formation (Table 3), whereas the presence or absence of eIF5B had no detectable effect on the kinetics of 43S complex formation (Table 2). These data indicate that eIF5B acts on a step after 43S complex formation, consistent with its proposed role in subunit joining (Trachsel et al., 1977; Benne & Hershey, 1978; Pestova et al., 2000).

Omission of eIF5 from the system had a more subtle effect than the omission of the other factors. When eIF5 was omitted from reactions carried out as described in Figure 5A, Scheme 2, the observed rate constant for complex formation was not significantly affected relative to the rate constant measured when eIF5 was present (Table 3). The amplitude of the reaction was markedly increased, however (Fig. 7A). The reason for this increase has yet to be determined. Interestingly, when the reactions were initiated without the P3 preincubation (Fig. 5A, Scheme 1), omission of eIF5 resulted in a more pronounced lag phase in the observed kinetics and an altered curve shape (Fig. 7B). The data are fit well with an equation describing an irreversible two-step process (see Materials and Methods), indicating a fourfold decrease in the observed rate constant of the first step with no significant affect on the second step ($k_1 = 0.67 \pm 0.08$ min^{-1} and $k_2 = 0.13 \pm 0.004$ min^{-1} in the presence of eIF5 compared to $k_1 = 0.16 \pm 0.03$ min^{-1} and $k_2 = 0.12 \pm 0.03$ min^{-1} in the absence of eIF5). These data suggest that eIF5 is involved in an early slow step on the pathway to initiation complex formation and that this step is complete by the end of the P3 preincubation whether or not eIF5 is present.

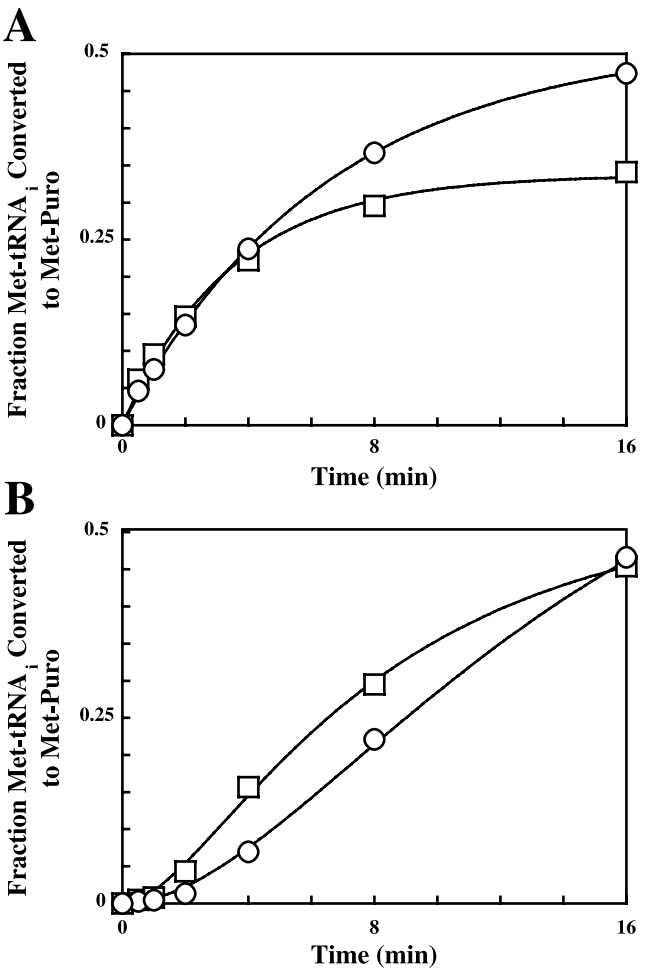

FIGURE 7. Omitting eIF5 from reactions slows the rate of some intermediate, rate limiting step without significantly affecting the rate of subsequent steps. **A**: Kinetics of Met-Puro reactions initiated as described in Figure 5A, Scheme 2 with or without eIF5. Data were fit with a single exponential (solid lines). The reaction carried out in the presence of saturating eIF5 (□) proceeded with an observed rate constant of 0.19 ± 0.02 min^{-1}, whereas the reaction carried out in the absence of added eIF5 (○) proceeded with an observed rate constant of 0.15 ± 0.004 min^{-1}. The errors given are the errors of the fits. **B**: Kinetics of reactions initiated by simultaneous addition of puromycin, ribosomes, model mRNA, eIF1, eIF1A, and eIF5B with or without eIF5 (Fig. 5A, Scheme 1). Reactions carried out in the absence of eIF5 (○) proceeded with observed rate constants of $k_1 = 0.16 \pm 0.03$ min^{-1} and $k_2 = 0.12 \pm 0.03$ min^{-1}, whereas reactions carried out in the presence of eIF5 (□) proceeded with observed rate constants of $k_1 = 0.67 \pm 0.08$ min^{-1} and $k_2 = 0.13 \pm 0.004$ min^{-1}. These rate constants are the averages of two independent experiments. The errors given are the mean deviations.

DISCUSSION

We have reconstituted yeast translation initiation in vitro using a minimal set of purified *S. cerevisiae* initiation factors and ribosomes. Using this system we have been able to examine the kinetics of steps in the assembly of translation initiation complexes in vitro, as well as the roles that individual components play in this intricate process. This new system should be a powerful addition to previously described reconstituted mammalian translation initiation systems (Trachsel et al., 1977; Benne & Hershey, 1978; Pestova et al., 1998, 2000) because of the ease and power of yeast genetics and molecular biology and it should provide a bridge between experiments performed in vivo and in vitro.

Many aspects of the current model for the assembly of an active initiation complex (Hershey & Merrick, 2000) are borne out in the reconstituted yeast system. This similar behavior to what had previously been found in other systems suggests that the reconstituted yeast system is recapitulating many of the central events in translation initiation common to all eukaryotes. For example, the formation of an active initiation complex de-

pends strongly on the presence of an mRNA containing an AUG codon and also requires the hydrolysis of GTP. GTP hydrolysis, however, is not required for formation of 43S complexes, consistent with the current model for initiation in which hydrolysis does not happen until after initiation codon recognition. Even more encouraging than these similarities, however, is the dependence of various steps in the system on the presence of initiation factors, discussed in more detail below. These dependencies suggest that this system should be useful for probing the molecular mechanisms used by the initiation factors to catalyze and coordinate the formation of active initiation complexes.

Testing the roles of the initiation factors

As described in the Results section, the formation of both 43S and 80S initiation complexes are completely dependent upon the presence of eIF2 in the system, as expected given the factor's central role in bringing Met-tRNA$_i$ onto the small ribosomal subunit during the initiation process (Hershey & Merrick, 2000). The loading of the eIF2•GTP•Met-tRNA$_i$ complex onto the 40S ribosomal subunit to form the 43S complex is strongly enhanced by the presence of saturating eIF1A (>100-fold). Using sucrose gradient sedimentation analysis, several groups previously reported a dependence of 43S complex formation on eIF1A in reconstituted mammalian systems (Trachsel et al., 1977; Benne & Hershey, 1978; Thomas et al., 1980a; Chaudhuri et al., 1997). Based on these observations, the generally accepted function of this factor is to assist ternary complex binding to the 40S subunit (Hershey & Merrick, 2000). Our data support this model.

eIF1 has also previously been reported to facilitate the formation of 43S complexes (Thomas et al., 1980b), although this effect has generally not been incorporated into more recent models for the pathway of eukaryotic translation initiation. In the yeast system described here, there is a strong dependence (~10-fold) of the observed rate constant for 43S formation on the presence of eIF1, consistent with these previous observations. Through genetic screens, yeast eIF1 (Sui1p) has also been shown to be involved in maintaining the fidelity of initiation codon selection (Yoon & Donahue, 1992), and in vitro experiments have implicated both eIF1 and eIF1A in the assembly of 43S complexes that are competent to scan the mRNA and locate the translational start site (Pestova et al., 1998). How these functions relate to eIF1 and eIF1A's facilitation of 43S complex formation itself is unclear at this point. Answering this question will require a thorough investigation of the molecular mechanics of the steps in the initiation pathway from 43S formation to initiation codon selection.

We also observed that the presence of eIF5B greatly stimulates (~10-fold) the formation of 80S initiation complexes but has no effect on the formation of 43S complexes. This behavior is consistent with eIF5B's proposed role in stimulating the subunit joining step of translation initiation (Trachsel et al., 1977; Benne & Hershey, 1978; Pestova et al., 2000).

In contrast to the easily detected effects of eIFs 1, 1A, 2, and 5B, the effect of eIF5 in this system is more subtle. eIF5 is thought to be a GTPase activating protein (GAP) for eIF2, and eIF5 mutants have been found that decrease the fidelity of initiation codon selection (Huang et al., 1997). Our data suggest that eIF5 acts in our system by accelerating a step after 43S formation but prior to the final rate limiting step. It also appears that given enough time (10 min), this eIF5-dependent step can be accomplished even in the absence of added eIF5. These data are consistent with a model (Fig. 8) in which eIF5 is involved in stimulating GTP hydrolysis by eIF2 to yield the 40S•mRNA•Met-tRNA$_i$ complex, as has been proposed previously (Hershey & Merrick, 2000). When saturating eIF5 is present, the rate constant for this step is $\geq$0.7 min^{-1} (Figs. 7B and 8). We cannot yet tell whether the step after ternary complex formation that has an observed rate constant of 0.7 min^{-1} in the presence of saturating eIF5 (Fig. 7B) is the eIF5-dependent step itself or some other step either before or after it (or a combination of steps). It should be noted, however, that 0.7 min^{-1} is close to the measured rate constant for 43S formation in the presence of GDPNP (0.4 $\pm$ 0.2 min^{-1}), and thus it is possible that the rate constant for the eIF5-dependent step increases by an order of magnitude or more when saturating eIF5 is added to the system, leaving 43S formation as the first slow step after ternary complex assembly. In the absence of added eIF5, the observed rate constant for the eIF5-dependent step decreases from $\geq$0.7 min^{-1} to 0.2 min^{-1}. This 0.2 min^{-1} observed rate constant may represent the intrinsic rate of GTP hydrolysis by eIF2 in the absence of eIF5 or there may be contaminating eIF5 already in the system (e.g., from the ribosomes or eIF2, both of which are purified from yeast), resulting in decreased dependence on added eIF5. eIF5 could not be detected in either the eIF2 or the ribosomes by western blotting using anti-eIF5 antibodies, however, arguing against this latter possibility (data not shown). In any event, the data strongly suggest that eIF5 does stimulate a step in the initiation process in this system after 43S complex formation but before the final rate limiting step (see "Towards a kinetic and thermodynamic framework for eukaryotic translation initiation" below).

One interesting difference between the results obtained in this work and those obtained previously using mammalian systems is the lack of dependence on eIF3 in the yeast system. Several different models could explain this observation. One possibility is that our eIF3 preparation is inactive. For example, our preparation shows diminished levels of the Nip1p subunit relative to the other subunits and the loosely associated Hcr1p

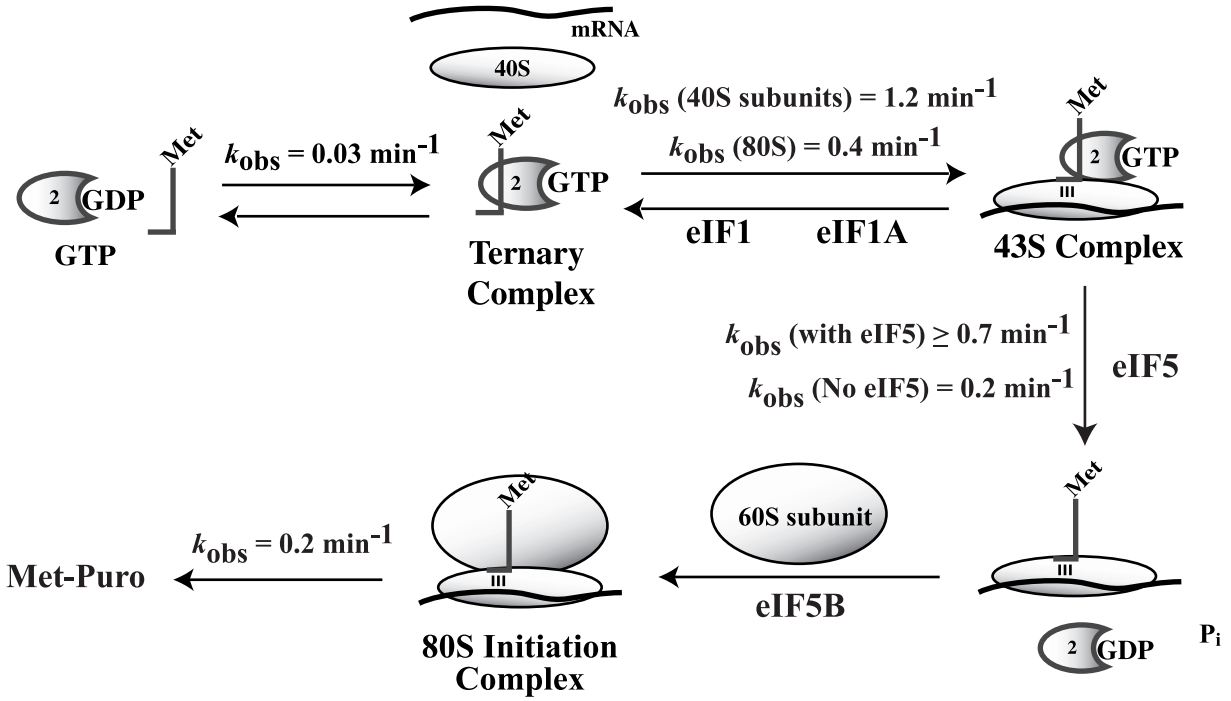

FIGURE 8. Summary of kinetic data. The slowest step in the system is the formation of the eIF2•GTP•Met-tRNA$_i$ ternary complex. Binding of the ternary complex to the 40S subunit to form the 43S complex is facilitated by eIF1 and eIF1A. The data suggest that eIF5 acts at a step after 43S complex formation but prior to the final rate limiting step, consistent with eIF5's proposed role as a GTPase activating protein for eIF2. As had been observed in mammalian systems, the presence of eIF5B is required for joining of the 40S and 60S subunits to give the 80S initiation complex. The final rate limiting step in the system has been tentatively assigned to the conversion of the 80S initiation complex to yield the Met-puromycin dipeptide. The reported rate constants are observed rate constants under the conditions used in these experiments.

subunit is not detectable by Coomassie staining (Fig. 1; Valasek et al., 2001). However, our eIF3 was able to rescue translation of luciferase mRNA in a heat-treated extract made from a yeast strain with a temperature-sensitive version of Prt1p (*prt1-1*; Phan et al., 1998) to the same extent as an independent preparation of eIF3 made from a strain that overexpresses all five core subunits of eIF3 (Phan et al., 2001; the addition of eIF3 increased the rate of luciferase production by 2.5-fold over background; both eIF3 samples were at ~0.2 μM, the highest achievable concentration with our eIF3 preparation; data not shown). As the *prt1-1* extracts have previously been shown to require the addition of at least the Prt1p-Nip1p-Tif32p subcomplex of eIF3 to restore translation of luciferase mRNA (Phan et al., 2001), these data suggest that these three subunits of our eIF3 preparation are active.

It is also possible that one or more of our components are contaminated with eIF3, the most likely candidates being the ribosomes or the eIF2. However, western blotting with antibodies against Tif32p, Prt1p, Tif34p, and Tif35p did not detect any of these subunits of eIF3 in our eIF2 preparation (data not shown). Bands just above background levels corresponding in size to Tif34p and Tif35p could be detected in our ribosome preparation, but no Tif32p or Prt1p could be detected (data not shown; we estimate that a concentration of 2 nM eIF3 in either the ribosomes or eIF2 would easily have been detectable in these experiments; this level of contamination would result in ≤0.2 nM eIF3 contamination in our reconstituted system). These data indicate that there is little if any contamination with eIF3 in our eIF2 and ribosome preparations, arguing against the possibility that such contamination accounts for the lack of eIF3 dependence observed in our system.

Another possibility is that eIF3 is involved in a step that is not rate limiting under our experimental conditions. For example, eIF3's main function might be to facilitate mRNA binding to the 40S subunit. In this case, it might have no effect in our system because of the unstructured nature of the mRNA template, which does not appear to require the mRNA binding and structure remodeling machinery of the eukaryotic translation initiation apparatus (Lorsch & Herschlag, 1999, and see below). Previous work with reconstituted mammalian systems has generally indicated that the most pronounced effect of eIF3 is to facilitate mRNA binding and that its effects on 43S complex formation are more modest (Trachsel et al., 1977; Benne & Hershey, 1978). It is also difficult to disentangle the effects eIF3 has on message binding from those it has on ternary complex binding because the two processes are likely coupled

(e.g., the endpoint of 43S formation is decreased two- to threefold in the absence of message in our system; see "Kinetics of 43S initiation complex formation can be monitored in the purified system" in Results). These questions can be further addressed when mRNA binding and structure remodeling events are recapitulated in this system (see below).

Towards a kinetic and thermodynamic framework for eukaryotic translation initiation

Using this reconstituted yeast translation initiation system, we have already been able to probe the observed rate constants for several of the key steps along the initiation pathway in vitro. The data we have generated thus far are summarized in Figure 8. It should be stressed that these data reflect the kinetics of the initiation process in this reconstituted system only and that the kinetics of initiation in vivo may be substantially different than what is observed here (see next section as well).

The slowest step in the system is the formation of the ternary eIF2•GTP•Met-tRNA$_i$ complex (0.03 min^{-1}), which is itself limited by the rate of GDP release from eIF2•GDP. This step is likely to take place much more rapidly in vivo because of the presence of the GDP:GTP exchange factor eIF2B. The binding of the ternary complex to the small ribosomal subunit to form the 43S complex proceeds over an order of magnitude more rapidly than ternary complex formation (0.4–1.2 min^{-1}). This step is followed by an eIF5-dependent step, possibly the hydrolysis of GTP by eIF2. We have not yet directly measured the rate constant for the subunit joining step, but initial experiments suggest it will be feasible to do so and that it is $>$0.1 min^{-1} (data not shown). The final slow step in the pathway, occurring with an observed rate constant of 0.2 min^{-1}, has been tentatively assigned to the conversion of the 80S initiation complex to give the Met-Puro dipeptide. This assignment was made because this observed rate constant does not change when the ternary complex and the remaining components of the system are incubated for 10 min prior to the addition of puromycin to initiate peptide bond formation (Fig. 5A,B). If a step involved in 80S complex assembly were responsible for this observed rate constant, it would be expected that incubation of all of the components of the system prior to initiation of the reaction with puromycin would alter the observed kinetics of the final slow step on the pathway to peptide bond formation. Some 80S complex would be formed during the incubation step and this 80S complex would react rapidly when puromycin was added, producing an observable fast phase of Met-Puro formation ($k_{obs} \gg$ 0.2 min^{-1}). Intermediate complexes that had not yet passed the slow step would produce a second slower phase of Met-Puro production with an observed rate constant of 0.2 min^{-1}. However, no fast phase is observed when puromycin is added after the 10-min preincubation and only a single exponential reaction with a k_{obs} of 0.2 min^{-1} is seen (Fig. 5B) suggesting that a step after 80S complex formation is the final rate limiting step. The scheme shown in Figure 8 represents the foundation for a more thorough kinetic and thermodynamic dissection of the initiation process using this reconstituted system.

Further development of the system

There are at least two shortcomings of our system that are worthy of note. First, it has been estimated that the observed rate constant for translation initiation in vivo is ~9 min^{-1} (Palmiter, 1975). This is over an order of magnitude higher than the rate limiting steps in our system. Thus, some further optimization of the system is warranted. It is possible that a key factor is missing from the system or that one of our components is not fully active. For example, the ribosomes may have been partially inactivated during preparation, perhaps as the result of pressure during centrifugation (Morley & Hershey, 1990). It is also possible that differences between the reaction conditions in vitro and the cellular milieu in vivo (e.g., decreased activity of water in vivo) are responsible for the differences in the rate constants.

Finally, to simplify the initial development of this system, we chose to use a minimal model mRNA. Because this model mRNA is small and is predicted to be unstructured, we reasoned that 5′ cap binding and mRNA unwinding would not be required with this message. In keeping with this expectation, all of the components thought to be involved in these steps of initiation (eIFs 4A, 4B, 4E, 4G, PAB, and ATP) are not required in the reconstituted system when the minimal mRNA is used. The 5′ cap structure and 3′ poly(A) tail are also not required for initiation on the minimal mRNA. The next challenges will be to build these mRNA binding and structural remodeling events into the reconstituted system using a natural mRNA as a template and to develop assays to probe the molecular mechanics of these key steps in the initiation process.

MATERIALS AND METHODS

Purification of yeast initiation factors

eIF1

The eIF1 gene (sui1) was cloned into the expression vector pTYB2 (New England Biolabs) and transformed into CodonPlus BL21 DE3 *E. coli* cells (Stratagene). Transformants were used to inoculate 5 mL of LB containing 50 μg/mL carbenicillin and 34 μg/mL chloramphenicol. After growth to saturation (overnight) at 37 °C, this culture was used to inoculate 1 L of LB containing 50 μg/mL carbenicillin and 34 μg/mL

chloramphenicol to a final OD_{600} of 0.1. After incubation of this culture at 37 °C until an OD_{600} of 0.4 was reached, expression was induced by addition of IPTG to a final concentration of 0.3 mM. The cells were grown at 16 °C for 20 h after induction, pelleted, and suspended in 20 mL of 150 mM KCl, 20 mM HEPES-NaOH, pH 8.0, 2 mM DTT, plus protease inhibitors (1 μg/mL leupetin, 1 μg/mL pepstatin, 1 μg/mL aprotinin, 1 mM benzamidine, 0.5 mM AEBSF). The cells were then lysed by passage twice through a French pressure cell and the lysate was clarified by centrifugation at 20,000 $\times$ *g* for 35 min at 4 °C. The clarified lysate was purified on a 1-mL column of chitin beads as described by the manufacturer (New England Biolabs). Fractions containing eIF1 were pooled and dialyzed against 20 mM HEPES-KOH, pH 7.6, 100 mM KOAc, 2 mM DTT, 10% glycerol. Purified eIF1 was aliquoted, flash frozen in liquid N_2, and stored at −80 °C.

eIF1A

eIF1A (Tif11p) was expressed as an N-terminal GST fusion protein from a pGEX-4T-1 vector (Amersham Pharmacia) in CodonPlus BL21 DE3 *E. coli* cells (Stratagene). A starter culture (75 mL) of LB containing 50 μg/mL carbenicillin and 34 μg/mL chloramphenicol was grown at 37 °C to an OD_{600} of 0.6 and stored at 4 °C overnight. The cells were then pelleted and resuspended in fresh LB and used to inoculate 2 L of LB plus 50 μg/mL carbenicillin. This culture was grown to an OD_{600} of 0.4, induced with a final concentration of 1 mM IPTG, and grown for an additional 4 h. Cells were pelleted and stored at −80 °C. The pellet was rapidly thawed and suspended in 50 mL of 150 mM KCl, 20 mM Tris-Cl, pH 7.6, 2 mM DTT, 10% glycerol (buffer A) plus protease inhibitors (as described above for eIF1) and the cells were lysed by two passes through a French pressure cell. Cellular debris was cleared by centrifugation at 17,000 $\times$ *g* for 20 min at 4 °C. The supernatant was applied to 3 mL of glutathione-agarose resin (Sigma) equilibrated in buffer A and incubated with gentle rotation for 1 h at 4 °C. The resin was then washed with six volumes of buffer A and the protein eluted with 50 mM Tris-Cl, pH 8.5, 50 mM glutathione. The fractions containing the eIF1A-GST fusion were made 150 mM in NaCl and 2.5 mM in $CaCl_2$ and 22 U of biotinylated thrombin (Novagen) were added to cleave the GST tag. The cleavage reaction was incubated at ambient temperature for 12 h followed by removal of the biotinylated thrombin using streptavidin agarose according to the manufacturer's protocol. The sample was then applied to a 5-mL HiTrap heparin column (Amersham Pharmacia) and eluted with a linear gradient from 0.15–1 M KCl (20 mM Tris-Cl, pH 7.6, 2 mM DTT, 10% glycerol) over 60 mL. eIF1A eluted at ~0.5 M KCl. The eIF1A-containing fractions were dialyzed against 20 mM HEPES-KOH, pH 7.6, 100 mM KOAc, 2 mM DTT, 10% glycerol. Purified eIF1A was aliquoted, flash frozen in liquid N_2, and stored at −80 °C.

eIF2

His-tagged eIF2 was overexpressed in yeast strain GP3511 and purified as described previously (Pavitt et al., 1998) with minor modifications. The cells were lysed using a French pressure cell rather than bead beating and the protein was further purified on a 1-mL UNO Q1 column (BioRad) following the Ni^{2+} and heparin chromatography steps. The protein was eluted from the UNO Q1 column using a linear gradient from 0.1–1 M KCl in buffer A.

eIF3

His-tagged eIF3 was expressed in yeast strain LPY201 and purified as described previously (Phan et al., 1998).

eIF5

N-terminally His-tagged eIF5 was expressed in *E. coli* as described above for eIF1A. The cell pellets were resuspended in nickel column loading buffer (NCLB; 20 mM Tris-Cl, pH 7.6, 500 mM KCl, 10 mM imidazole, 10 mM β-mercaptoethanol, 10% glycerol) plus protease inhibitors (as for eIF1) and lysed in a French pressure cell. The lysate was cleared as described for eIF1, applied to 5 mL of Ni^{2+}-NTA agarose (Qiagen), and incubated at 4 °C with gentle rotation for 2 h. The resin was washed with 10 column volumes of NCLB and then the protein was eluted with 3 column volumes of NCLB plus 250 mM imidazole. The eluted protein was further purified on a 100-mL Superose 12 gel filtration column (1.6 $\times$ 50 cm) equilibrated in buffer A plus protease inhibitors. The fractions containing eIF5 were then loaded onto a 5-mL HiTrap heparin column and eluted as described for eIF1A. Fractions containing eIF5 were pooled and dialyzed against buffer A plus protease inhibitors and applied to a 1-mL UNO Q1 column and eluted as described above for eIF2. The purified protein was dialyzed and stored as for eIF1A.

eIF5B

An N-terminally truncated form of yeast eIF5B (residues 396–1002), which complements the eIF5B knockout in vivo (Choi et al., 1998), was expressed as a GST fusion from plasmid pC848, a derivative of pGEX-4T-2 (gift of T. Dever). The protein was expressed and purified according to the procedure described for eIF1A above, including cleavage of the GST tag. Between the glutathione sepharose and heparin chromatography steps, an additional fractionation over a 1-mL UNO Q1 column was used, as described above for eIF2 purification.

Protein concentration determination

All protein concentrations were determined using the Bio-Rad Protein Assay (Bio-Rad) microassay procedure as described by the manufacturer. Bovine serum albumin (BSA) was used as the standard in all concentration determinations.

Ribosomes

Rationale

An initial problem we had in making active yeast ribosomes was an uncharacterized group of nucleases that cosediment with the ribosomes and are activated during the high salt wash step of standard ribosome purification protocols. These nucleases degrade the ribosomal RNA and any exogenous

RNA added to the ribosomes (e.g., mRNA), resulting in preparations with no detectable translational activity. Several different yeast genotypes were found to have these nucleases, including a pep4$^-$ strain and an xrn1$^-$, pep4$^-$ strain (data not shown). It was found, however, that inclusion of heparin (1 mg/mL) in all buffers used through the high salt wash step (see below) removed the nucleases. The rRNA of the resulting preparations is >80% full length, compared to <10% full length when the purification is carried out in the absence of heparin (data not shown). Furthermore, exogenous mRNA added to ribosomes prepared in this manner is stable for several hours. Finally, these ribosomes are active (see Results), and heparin was thus routinely included in the buffers used for 80S ribosome preparations. It was also found that deletion of four Rex exonuclease genes (Rex1–4; van Hoof et al., 2000) greatly reduced the nuclease contamination problem and active ribosomes could be made from this yeast strain (data not shown). However, because several of the Rex exonucleases have been implicated in 5S and 5.8S rRNA processing (van Hoof et al., 2000), we chose not to use these ribosomes for our experiments.

Interestingly, although no heparin was employed during the purification of 40S subunits, the resulting 40S subunits were fully competent to form 43S complexes when compared to 80S preparations (see Results). The reasons for this are not yet clear, although it should be noted that the 60S subunits obtained using the subunit purification protocol could not be assembled into active complexes.

Salt-washed 80S ribosome preparation

A 5-mL culture of *S. cerevisiae* strain YRP840 (Mat a, Leu2-3 112, His4-53a, Trp1, Ura3-52, cup1::LEU/PGK1pG/MFA2pG; van Hoof et al., 2000) was grown overnight at 30 °C in YPD complete medium. Three 1-L batches of YPD media were inoculated with 1 mL each of the overnight culture and incubated at 30 °C overnight until an OD_{595} of ~2.6 was reached. The yeast were then cooled on ice for at least 1 h and the cells were centrifuged at 6,000 × *g* for 10 min at 4 °C. The yeast pellets were resuspended in a total volume of 30 mL of ribosome buffer plus protease inhibitors and heparin (100 mM KOAc, 20 mM HEPES-KOH, pH 7.6, 2.5 mM $Mg(OAc)_2$, 1 mg/mL heparin, 2 mM DTT, 10 μg/mL leupetin, 10 μg/mL pepstatin, 10 μg/mL aprotinin, 10 mM benzamidine, 5 mM AEBSF). The cells were lysed by passage twice through a French pressure cell. The resulting lysate was centrifuged at 17,000 × *g* for 30 min at 4 °C. After centrifugation, the supernatant was carefully removed while avoiding the lipids at the top and then centrifuged again in a Beckman Optima TLX tabletop ultracentrifuge using a TLA 100.3 rotor at 400,000 × *g* for 20 min at 4 °C. The supernatant was removed and the pellets washed with 0.5 mL of ribosome buffer plus heparin. The pellets were resuspended in a total of 18 mL of high salt buffer (100 mM KOAc, 20 mM HEPES-KOH, pH 7.6, 2.5 mM $Mg(OAc)_2$, 1 mg/mL heparin, 500 mM KCL, 2 mM DTT) and stirred gently on ice for 30–60 min. Following the high salt wash, the solution was placed in 1.5-mL tubes and centrifuged at 14,000 rpm in a bench top microcentrifuge for 10 min at 4 °C to clear insoluble material. The supernatant was removed and placed in new 1.5-mL tubes and recentrifuged at 14,000 rpm for 10 min at 4 °C. This procedure was repeated for a total of four centrifuge spins. The resulting supernatant was divided into aliquots of 2.75 mL and each aliquot was placed on top of 0.25 mL of sucrose cushion (100 mM KOAc, 20 mM HEPES-KOH, pH 7.6, 2.5 mM $Mg(OAc)_2$, 500 mM KCL, 1 M sucrose, 2 mM DTT) and centrifuged in the table top ultracentrifuge at 400,000 × *g* for 20 min at 4 °C. Following centrifugation, the supernatant was removed and the pellets were quickly washed with 0.5 mL of ribosome storage buffer (100 mM KOAc, 20 mM HEPES-KOH, pH 7.6, 2.5 mM $Mg(OAc)_2$, 250 mM sucrose, 2 mM DTT). The pellets were resuspended in ribosome storage buffer, flash frozen in liquid N_2 and stored at −80 °C.

40S ribosomal subunit preparation

A 5-mL culture of *S. cerevisiae* strain F353 (Matα, Ura3-52, Trp1, Leu2-D1, His3-Δ200, pep4::HIS3, prb1-Δ1.6, can1, GAL+; gift of T. Dever) in YPD was grown at 30 °C overnight and then used to inoculate 3 L of YPD (1 mL overnight culture per 1 L YPD). This culture was grown overnight at 30 °C to an OD_{600} of 1.5–2.0 and then pelleted by centrifugation at 6,000 × *g* for 10 min at 4 °C. The pellets were suspended in an equal volume of breaking buffer (50 mM KCl, 10 mM $MgCl_2$, 1 mM DTT, 0.1 mM EDTA, 20 mM Tris-HCl, pH 7.6, plus protease inhibitors as described above under *80S*) and lysed by passage twice through a French pressure cell. The lysate was clarified by centrifugation at 14,000 × *g* for 30 min at 4 °C. Crude ribosomes were then pelleted from the resulting supernatant by centrifugation at 100,000 × *g* for 3 h at 4 °C in a Beckman ultracentrifuge using a 70.1 Ti rotor. The resulting pellet was dissolved in 10 mL ribosomal salt wash buffer (1 mM DTT, 0.1 mM EDTA, 0.25 M sucrose, 0.5 M KCl, 20 mM Tris-HCl, pH 7.6) by gentle stirring for 1 h. This solution was subjected to centrifugation at 100,000 × *g* for 4 h at 4 °C. The pellet was suspended in a small volume of subunit buffer (50 mM HEPES-KOH, pH 7.4, 2 mM $MgCl_2$, 500 mM KCl) and the volume was adjusted to give 50 OD_{260}/mL. Puromycin was added to a final concentration of 1 mM, and the mixture was incubated on ice for 15 min, at 37 °C for 10 min and then returned to ice. Samples (1 mL) were then loaded onto 5–20% sucrose gradients and centrifuged using a SW28 rotor at 76,000 × *g* for 9 h at 4 °C. The gradients were fractionated using a Brandel gradient fractionator and fractions containing 40S subunits were pooled. The pooled fractions were diluted twofold with water and centrifuged using a Type 50.2 Ti rotor at 145,000 × *g* for 20.5 h at 4 °C. The resulting pellets were suspended in subunit storage buffer (20 mM Tris-HCl, pH 7.6, 0.25 M sucrose, 1 mM DTT, 0.2 mM EDTA, 10 mM KCl, 1 mM $MgCl_2$), aliquoted, flash frozen in liquid N_2, and stored at −80 °C.

Ribosome concentration determination

Purified 80S ribosome and 40S subunit concentrations were determined by measuring the absorbance at 260 nm and using extinction coefficients of 5×10^7 cm^{-1} M^{-1} and 2×10^7 cm^{-1} M^{-1} for 80S ribosomes and 40S subunits, respectively (Matasova et al., 1991).

Model mRNA template

The model mRNA (5′-GGAA[UC]$_7$UAUG[CU]$_{10}$C-3′) was synthesized by T7 polymerase run-off transcription and purified

by denaturing PAGE as previously described (Lorsch & Herschlag, 1999).

Charged tRNA

Yeast methionyl-tRNA$_i$ in yeast total tRNA was charged with [^{35}S]methionine using a crude preparation of *E. coli* tRNA synthetases as previously described (Lorsch & Herschlag, 1999).

Kinetic assays

Standard reaction conditions

All assays (43S and Met-Puro) were performed with the optimized component concentrations given in Table 1. The final buffer conditions of the reactions in both assays was 38 mM HEPES-KOH, pH 7.4, 135 mM KOAc, 3.25 mM $Mg(OAc)_2$, 2.7 mM DTT, 25 mM sucrose, and 2.5% glycerol. These conditions include contributions from the factors and ribosomes.

Met-Puro assay

Met-Puro assays were carried out essentially as previously described (Lorsch & Herschlag, 1999) with the exception that the final glycerol concentration in the reactions was typically 2.5%. Reactions were analyzed by cation-exchange TLC followed by PhosphorImaging (Molecular Dynamics), as described previously (Lorsch & Herschlag, 1999).

43S complex formation assay

43S complex formation assays were carried out essentially as previously described (Lorsch & Herschlag, 1999) with some modifications. First, 4% polyacrylamide gels were prepared with 40 mM Tris-HCl, pH 6.0, 20 mM potassium acetate, 2.5 mM Mg^{2+}. The low pH of the gel was found to reduce deacylation of the free ^{35}S-Met-tRNA$_i$ as it runs through the gel. Control experiments showed no difference in the radioactivity found in complexes observed in pH 6.0 gels compared with those observed in pH 7.4 gels, indicating that the change in pH does not affect the amount of 43S complex once it has entered the gel (data not shown). Second, gels were typically run at 20 W such that the sample loaded first was run on the gel for 90 min or less and the sample loaded last was run for at least 40 min (see staggering of free tRNA in Fig. 4). These conditions allow the 43S complex to be sufficiently resolved without allowing the free ^{35}S-Met-tRNA$_i$ to run off the gel. The eIF2•GTP•Met-tRNA$_i$ ternary complex apparently dissociates rapidly upon entering the gel; multiple attempts to detect this complex using this and other native gel systems were unsuccessful and only free ^{35}S-Met-tRNA$_i$ was observed (data not shown). In contrast, nitrocellulose filter binding assays can readily detect the formation of the ternary complex using our purified eIF2 and give values for the dissociation constant for Met-tRNA$_i$ of ~10 nM, consistent with previously reported measurements (L. Kapp & J.R. Lorsch, unpubl.; Erickson & Hannig, 1996).

Upon completion of the experiments, the gels were wrapped in plastic wrap and placed on PhosphorImager screens that were then exposed overnight at −20 °C. The entire cassette was wrapped in plastic wrap before being placed at −20 °C to prevent moisture from affecting the screens. The cassettes were allowed to reach room temperature before the screens were removed and scanned.

Varying the running times of 43S complexes in native gels by several-fold did not affect the amount of 43S complex observed (data not shown), indicating that dissociation of 43S complexes does not occur at a significant rate once the complex has run into the gel matrix.

General kinetics

Analysis of kinetic data was carried out as described previously (Lorsch & Herschlag, 1999). All fits were performed using KaleidaGraph software (Synergy Software). Unless otherwise indicated, observed rate constants and relative rate constants are reported as the averages of two or more experiments and the errors reported are the mean deviations. The rate constants reported are observed pseudo-first-order rate constants (k_{obs}) under the conditions of the experiments and do not necessarily reflect the molecularity of the processes involved.

When experiments showed pseudo-first-order kinetics (i.e., experiments with the chase of unlabeled Met-tRNA$_i$), observed rate constants were obtained by fitting data to a single exponential equation, $A(1 - \exp(-kt))$, in which A is the amplitude and k is the observed rate constant. Data from experiments showing biphasic behavior were fit to a double exponential equation, $(A_1(1 - \exp(-k_1t)) + A_2(1 - \exp(-k_2t))$, in which A_1 and A_2 are the amplitudes and k_1 and k_2 are the observed rate constants for the two phases. In the instances when the double exponential fit was utilized, the first (fast) phase of the fit was used to determine the k_{obs} for the step(s) being monitored. In experiments that were done both with and without a chase, the k_{rel} values (Tables 2 and 3) determined either way were very similar (variation <2-fold). Data not fit with either of the previous equations was fit to an equation describing a two-step irreversible process, $A(1 + 1/k_1 + k_2[k_2\exp(-k_1t) - k_1\exp(-k_2t)]$ (Fersht, 1985; Lorsch & Herschlag, 1999). This is the simplest model that accounts well for the observed kinetics, although no experiments have yet been done to directly probe the rate constants for reverse reaction steps in this system. However, 43S complex formation goes essentially to completion, indicating that the overall forward rate for this step is considerably greater than the reverse rate. It should also be emphasized that all reported rate constants are observed rate constants for the process or processes being probed and likely do not represent fundamental rate constants for individual steps but rather reflect the sums of multiple rate constants.

When the rate of a step in the initiation process was slowed by lowering the concentration of a key component, changes in the endpoint of the reaction were often observed as well. This effect is most likely due to a competing process (or processes) that is unaffected by the change in component concentration, such as deacylation of Met-tRNA$_i$ or inactivation of factors or ribosomes. The measured k_{obs} values were corrected for these differing endpoints as previously described (Lorsch & Herschlag, 1999).

Relative rate constants and estimation of errors

The k_{obs} values from identical experiments carried out on different days varied by as much as twofold, resulting in large mean deviations in k_{obs} values (Tables 2 and 3). The variation was significantly smaller when the experiments were carried out side by side and seemed to correlate with different preparations of reagents (i.e., ribosomes, eIFs, mRNA, and Met-tRNA$_i$). Therefore, the observed rate constants for component omission experiments were normalized to the observed rate constants of positive control reactions (containing all components) carried out on the same day with the same reagents in order to obtain relative rate constants (k_{rel}). The numbers presented in Tables 2 and 3 represent the mean values of two or more k_{rel}s from independent experiments unless otherwise indicated. In contrast to the significant variation in the k_{obs} values, the k_{rel} values were more consistent from experiment to experiment (Tables 2 and 3).

ACKNOWLEDGMENTS

We are grateful to Tom Dever for advice, reagents, and providing us with the protocol for making 40S ribosomal subunits from yeast; to Rachel Green for advice and discussions; and to Roy Parker for the Rex1−4 deletion strain. We are also grateful to John Hershey and John McCarthy for encouragement in the early stages of this work. We thank Lee Kapp and Jeremy Berg for comments on the manuscript. D.M. is a National Science Foundation Predoctoral Fellow. This work was funded in part by grants from the National Institutes of Health and the Howard Hughes Medical Institute.

Received December 4, 2001; returned for revision December 17, 2001; revised manuscript received December 21, 2001

REFERENCES

Benne R, Hershey JWB. 1978. The mechanism of action of protein synthesis initiation factors from rabbit reticulocytes. *J Biol Chem 253*:3078–3087.

Chaudhuri J, Chowdhury D, Maitra U. 1999. Distinct functions of eukaryotic translation initiation factors eIF1A and eIF3 in the formation of the 40S ribosomal preinitiation complex. *J Biol Chem 273*:17975–17980.

Chaudhuri J, Si K, Maitra U. 1997. Function of eukaryotic translation initiation factor 1A (eIF1A) (formerly called eIF-4C) in initiation of protein synthesis. *J Biol Chem 272*:7883–7891.

Choi SK, Lee JH, Zoll WL, Merrick WC, Dever TE. 1998. Promotion of met-tRNAiMet binding to ribosomes by yIF2, a bacterial IF2 homolog in yeast. *Science 280*:1757–1760.

Erickson FL, Hannig EM. 1996. Ligand interactions with eukaryotic translation initiation factor 2: Role of the γ-subunit. *EMBO J 15*:6311−6320.

Fersht A. 1985. *Enzyme structure and mechanism*. New York: WH Freeman and Co.

Hershey JWB, Merrick WC. 2000. Pathway and mechanism of initiation of protein synthesis. In: Sonenberg N, Hershey JWB, Mathews MB, eds. *Translational control of gene expression*. Cold Spring Harbor, New York: Cold Spring Harbor Laboratory Press. pp 33–88.

Huang H, Yoon H, Hannig EM, Dohanue TF. 1997. GTP hydrolysis controls stringent selection of the AUG start codon during translation initiation in *Saccharomyces cerevisiae*. *Genes & Dev 11*:2396–2413.

Johnson AE, Adkins HJ. 1984. Glycerol, sucrose, and other diol-containing reagents are not inert components in in vitro incubations containing aminoacyl-tRNA. *Anal Biochem 137*:351–359.

Lorsch JR, Herschlag D. 1999. Kinetic dissection of fundamental processes of eukaryotic translation initiation in vitro. *EMBO J 18*:6705−6717.

Matasova NB, Myltseva SV, Zenkova MA, Graifer DM, Vladimirov SN, Karpova GG. 1991. Isolation of ribosomal subunits containing intact rRNA from human placenta: Estimation of functional activity of 80S ribosomes. *Anal Biochem 198*:219–223.

Morley SJ, Hershey JWB. 1990. A fractionated reticulocyte lysate retains high efficiency for protein synthesis. *Biochimie 72*:259–264.

Nika J, Yang W, Pavitt GD, Hinnebusch AG, Hannig EM. 2000. Purification and kinetic analysis of eIF2B from *Saccharomyces cerevisiae*. *J Biol Chem 275*. 26011–26017.

Palmiter RD. 1975. Quantitation of parameters that determine the rate of ovalbumin synthesis. *Cell 4*:189–197.

Pavitt GD, Ramaiah KV, Kimball SR, Hinnebusch AG. 1998. eIF2 independently binds two distinct eIF2B subcomplexes that catalyze and regulate guanine-nucleotide exchange. *Genes & Dev 12*:514–526.

Pestova TV, Borukhov SI, Hellen CUT. 1998. Eukaryotic ribosomes require initiation factors 1 and 1A to locate initiation codons. *Nature 394*:854–859.

Pestova TV, Lomakin IB, Lee JH, Choi SK, Dever TE, Hellen CU. 2000. The joining of ribosomal subunits in eukaryotes requires eIF5B. *Nature 403*:332–335.

Phan L, Schoenfeld LW, Valasek L, Nielsen KH, Hinnebusch AG. 2001. A subcomplex of three eIF3 subunits binds eIF1 and eIF5 and stimulates ribosome binding of mRNA and tRNA(i)(Met). *EMBO J 20*:2954–2965.

Phan L, Zhang X, Asano K, Anderson J, Vornlocher HP, Greenberg JR, Qin J, Hinnebusch AG. 1998. Identification of a translation initiation factor 3 (eIF3) core complex, conserved in yeast and mammals, that interacts with eIF5. *Mol Cell Biol 18*:4935−4946.

Rosa MD, Sigler PB. 1977. Isolation and characterization of two methionine:tRNA ligases from wheat germ. *Eur J Biochem 78*:141–151.

Saenger W. 1984. *Principles of nucleic acid structure*. New York: Springer-Verlag.

Thomas A, Goumans H, Voorma HO, Benne R. 1980a. The mechanism of action of eukaryotic initiation factor 4C in protein synthesis. *Eur J Biochem 107*:39−45.

Thomas A, Spann W, Van Steeg H, Voorma HO, Benne R. 1980b. Mode of action of protein synthesis initiation factor eIF-1 from rabbit reticulocytes. *FEBS Lett 116*:67–71.

Trachsel H, Erni B, Schreier MH, Staehelin T. 1977. Initiation of mammalian protein synthesis. II. The assembly of the initiation complex with purified initiation factors. *J Mol Biol 116*:755–767.

Valasek L, Phan L, Schoenfeld LW, Valaskova V, Hinnebusch AG. 2001. Related eIF3 subunits TIF32 and HCR1 interact with an RNA recognition motif in PRT1 required for eIF3 integrity and ribosome binding. *EMBO J 20*:891–904.

van Hoof A, Lennertz P, Parker R. 2000. Three conserved members of the RNase D family have unique and overlapping functions in the processing of 5S, 5.8S, U4, U5, RNase MRP and RNase P RNAs in yeast. *EMBO J 19*:1357–1365.

Yoon HJ, Donahue TF. 1992. The suil suppressor locus in *Saccharomyces cerevisiae* encodes a translation factor that functions during tRNA(iMet) recognition of the start codon. *Mol Cell Biol 12*:248–260.